Supporting Information for "Is the relation between the solar wind dynamic pressure and the magnetopause standoff distance so straightforward?"

A. A. Samsonov[1], Y. V. Bogdanova[2], G. Branduardi-Raymont[1], D. G. Sibeck[3], G. Tóth[4]

[1]Mullard Space Science Laboratory, University College London, UK

[2]RAL Space,Rutherford Appleton Laboratory, Science and Technology Facilities Council, UK

[3]NASA, Goddard Space Flight Center, Greenbelt, MD, USA

[4]Department of Climate and Space, University of Michigan, Ann Arbor, Michigan, USA

Contents of this file

Magnetopause reconnection rate S1

We estimate the magnetopause reconnection rate R in MHD simulations using the expression initially suggested by Cassak and Shay (2007) and applied for MHD simulations in purely southward IMF cases (Borovsky et al., 2008) and for arbitrary magnetic shear angles θ (the angle between magnetic field directions on the inner and outer boundaries of

Corresponding author: A. A. Samsonov, Mullard Space Science Laboratory, University College London, UK. (a.samsonov@ucl.ac.uk)

the magnetopause current layer) (Borovsky & Birn, 2014). We use the following formula for the absolute reconnection rate (in units of electric field)

$$R = 0.2\mu_0^{-1/2}(B_s B_m)^{3/2}(B_s\rho_m + B_m\rho_s)^{-1/2}(B_s + B_m)^{-1/2} * \sin^2(\theta/2), \quad (1)$$

where indices s and m indicate magnetic fields and densities on the magnetosheath and magnetospheric sides of the magnetopause current (reconnection) layer.

The reconnection rate may slightly depend on the method of fixing the boundaries of the current layer therefore we include Figure S1 which illustrates our approach. Below we use two high resolution runs with a maximal grid resolution 1/16 R_E around the subsolar magnetopause. Figure S1 shows electric field and current density profiles along the Sun-Earth line in three times with different solar wind dynamic pressure. Large peaks of the electric current density correspond to the magnetopause, and small peaks correspond to the bow shock. Vertical dotted lines indicate the boundary points on both sides of the current layers determined by condition J=0.15 J_{MAX} where J_{MAX} is the maximal current density at the subsolar magnetopause. Although this definition is not precise, but we can use this condition as long as it keeps the same in both runs for all times.

In Figure S2, we show temporal variations of the electric field, absolute reconnection rate, inflow velocity, and the reconnection rate normalized to the solar wind electric field in both runs at the outer boundary of the magnetopause current layer. Blue lines on the top panels correspond to the total solar wind electric field upstream of the bow shock. At the beginning of the runs, both the electric fields and absolute reconnection rates are about the same in both runs (or even a little smaller in the velocity run since the beginning electric field is weaker there). However, both Ey and R increase in the velocity run in response to increase in the solar wind electric field (upper right panel). At the end of

the runs with velocity increase, both Ey and R is about 2.5 times higher than those in the run with density increase (the driving solar wind electric field is 2.45 times higher in the velocity run). The reconnection rates normalized to the solar wind electric field (bottom panel) in the both case are very similar and slightly decrease from about 0.55 to 0.4 during the runs. The normalized reconnection rate in Borovsky et al. (2008) in their simulation A (a high Mach Alfven number case, $R/Ey_{SW} \simeq$0.5-0.6) is about the same as in our runs.

We should note that the Mach Alfven numbers M_A are the same in the density and velocity runs as long as we keep the same solar wind dynamic pressure and magnetic field because $M_A = V/V_A \sim \sqrt{P_d}/B_{SW}$. Using these simulations we can conclude that the magnetopause reconnection rate is proportional to the solar wind electric field, and since the E_{SW} is higher in the velocity run we obtain a higher absolute reconnection rate.

Temporal variations of the cross polar cap potential and magnetospheric magnetic field S2

Figures S3 and S4 show temporal variations of the cross polar cap potential and magnetospheric magnetic field at the subsolar geosynchronous point. The format of the figure is the same as in Figure 2. The left and right panels correspond to the northward and southward IMF cases, blue and red lines mark the runs with density and velocity increases respectively. The figures are discussed in the main part.

References

Borovsky, J. E., & Birn, J. (2014). The solar wind electric field does not control the dayside reconnection rate. *Journal of Geophysical Research: Space Physics*, *119*(2), 751-760. doi: 10.1002/2013JA019193

Borovsky, J. E., Hesse, M., Birn, J., & Kuznetsova, M. (2008). What determines the reconnection rate at the dayside magnetosphere? *Journal of Geophysical Research: Space Physics*, *113*(A7). doi: 10.1029/2007JA012645

Cassak, P. A., & Shay, M. A. (2007). Scaling of asymmetric magnetic reconnection: General theory and collisional simulations. *Physics of Plasmas*, *14*(10), 102114. doi: 10.1063/1.2795630

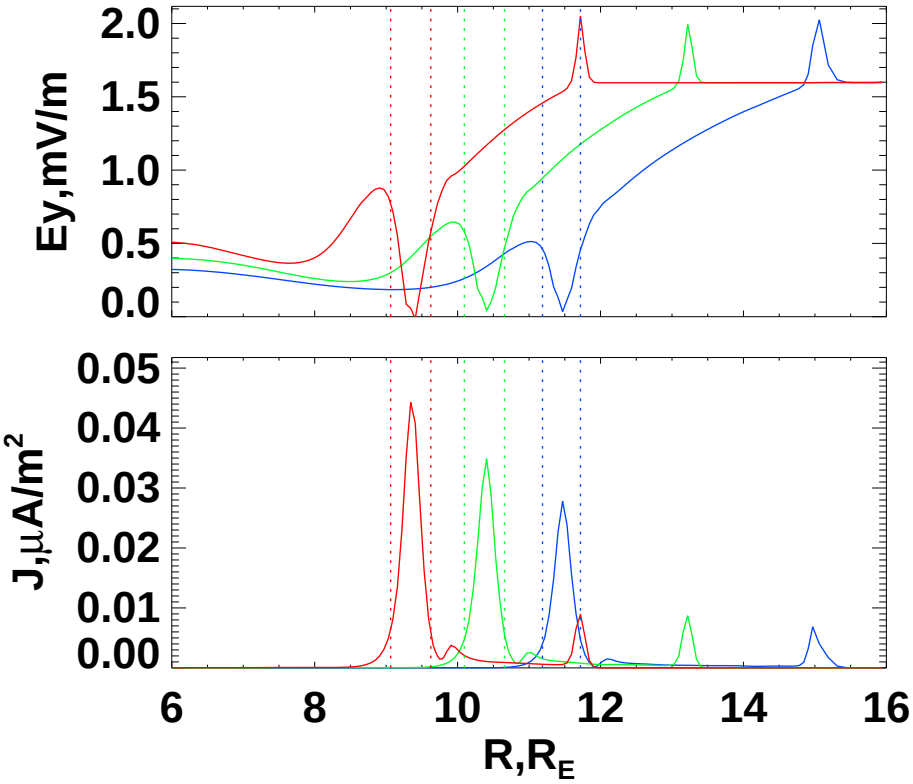

Figure S1. *Ey* electric field and electric current density profiles along the Sun-Earth line at t=03:00 (blue), 04:00 (green), and 05:00 (red).

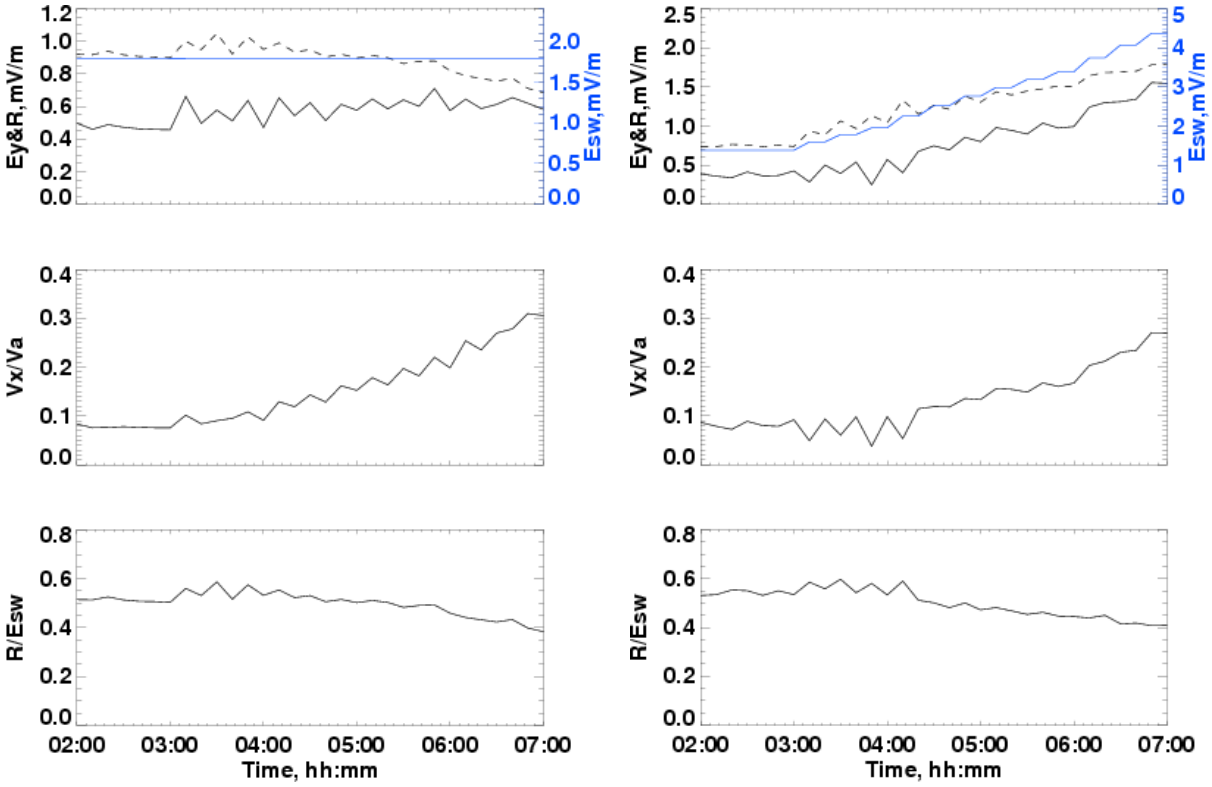

Figure S2. Top panel: Ey electric field (solid line) and reconnection rate (dashed line) at the outer boundary of the magnetopause current layer (or inflow region of the reconnection site), and the total solar wind electric field Esw (blue line); middle panel: Vx normalized to the Alfven velocity; bottom panel: reconnection rate normalized to the solar wind electric field. Results for the run with density increase shown on the left-hand side and for the run with velocity increase shown on the right-hand side.

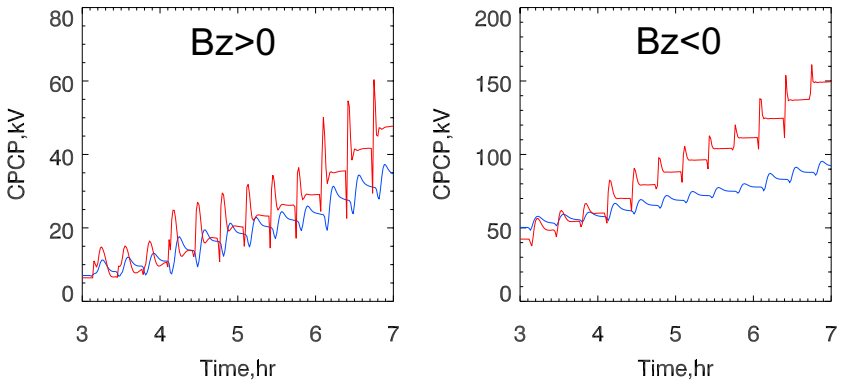

Figure S3. Temporal variations of the cross polar cap potential for northward (left panel) and southward (right panel) IMF, for the density (blue lines) and velocity (red lines) increases.

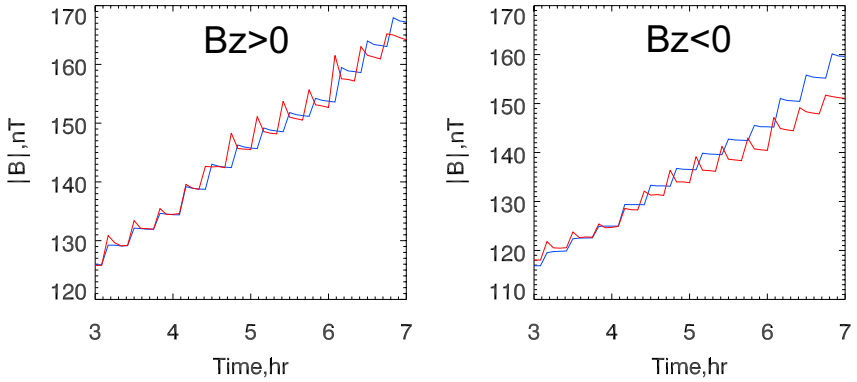

Figure S4. Temporal variations of the magnetic field magnitude at $x = 6.6$ R_E. The format is the same as in Figure S3.